Fine tuning of σ^E activation suppresses multiple assembly-defective mutations in *Escherichia coli*

Elizabeth M. Hart[a], Aileen O'Connell[a,b], Kimberly Tang[a], Joseph S. Wzorek[c,d], Marcin Grabowicz[a,e,f,g], Daniel Kahne[c], Thomas J. Silhavy[a#]

[a] Department of Molecular Biology, Princeton University, Princeton, NJ, 08540

[b] Laboratory of Virology and Infectious Disease, The Rockefeller University, 1230 York Avenue, Box 64, New York, NY, 10065

[c] Department of Chemistry and Chemical Biology, Harvard University, Cambridge, MA, 02138

[d] Novartis Institute for BioMedical Research, Inc., Cambridge, MA, 02139

[e] Emory Antibiotic Resistance Center, Emory University School of Medicine, Atlanta, GA, 30322

[f] Department of Microbiology and Immunology, Emory University School of Medicine, Atlanta, GA, 30322

[g] Division of Infectious Disease, Department of Medicine, Emory University School of Medicine, Atlanta, GA, 30322

Running title: Enhanced σ^E signaling counters outer membrane defects

Address correspondence to:
Thomas J. Silhavy
tsilhavy@princeton.edu

Abstract

The Gram-negative outer membrane (OM) is a selectively permeable asymmetric bilayer that allows vital nutrients to diffuse into the cell but prevents toxins and hydrophobic molecules from entering. Functionally and structurally diverse β-barrel outer membrane proteins (OMPs) build and maintain the permeability barrier, making the assembly of OMPs crucial for cell viability. In this work, we characterize an assembly-defective mutant of the maltoporin LamB, *lamB*$_{G439D}$. We show that the folding defect of LamB^{G439D} results in an accumulation of unfolded substrate that is toxic to the cell when the periplasmic protease DegP is removed. Selection for suppressors of this toxicity identified the novel mutant *degS*$_{A323E}$ allele. The mutant DegS^{A323E} protein contains an amino acid substitution at the PDZ/protease domain interface that results in a partially activated conformation of this protein. This activation increases basal levels of downstream σ^E stress response signaling. Furthermore, the enhanced σ^E activity of *degS*$_{A323E}$ suppresses a number of other assembly-defective conditions without exhibiting the toxicity associated with high levels of σ^E activity. We propose that the increased basal levels of σ^E signaling primes the cell to respond to envelope stress before OMP assembly defects threaten cell viability. This finding addresses the importance of envelope stress responses in monitoring the OMP assembly process and underpins the critical balance between envelope defects and stress response activation.

Importance

Gram-negative bacteria, such as *Escherichia coli*, inhabit a natural environment that is prone to flux. In order to cope with shifting growth conditions and the changing availability of nutrients, cells must be capable of quickly responding to stress. Stress response pathways allow

cells to rapidly shift gene expression profiles to ensure survival in this unpredictable environment. Here, we describe a mutant that partially activates the σ^E stress response pathway. The elevated basal level of this stress response allows the cell to quickly respond to overwhelming stress to ensure cell survival.

Introduction

The outer membrane (OM) of Gram-negative bacteria functions as a robust permeability barrier that selectively allows nutrients into the cell but prevents harmful molecules, such as antibiotics, from entering. Due to this critical balance, the biogenesis of the OM is a precisely regulated process that is essential for cell viability. The main functions of the OM, namely the passage of nutrients, the efflux of toxins, and the maintenance of membrane integrity, are carried out by integral β-barrel outer membrane proteins (OMPs). As such, defects in OMP assembly disrupt the selectivity of the permeability barrier and leave the cell vulnerable to antibiotics and other environmental threats (1, 2).

The early stages of the OMP assembly pathway have been extensively characterized over the past five decades. Briefly, precursor OMPs are transported across the inner membrane (IM) by the Sec translocon (3, 4). Chaperones, such as SurA, bind the OMP at the periplasmic face of the IM and ferry the processed, mature protein across the periplasm to the OM. During transport, SurA maintains the OMP in an unfolded state in order to prevent aggregation and misfolding in the oxidizing environment of the periplasm. The unfolded OMP is delivered to the heteropentomeric β-barrel assembly machine (Bam complex) and is assembled into the OM (5, 6). The mechanism by which the Bam complex interacts with and folds OMPs remains poorly understood.

Folding defects, translational error, or conditions that disrupt protein assembly can result in OMPs falling off of the assembly pathway and misfolding in the periplasm. Unchecked, this accumulation of unfolded proteins will lead to cell death (7, 8). The σ^E stress response monitors the cell for toxic aggregates and alters gene expression in response. In wild-type cells, OMP assembly is incredibly efficient and unfolded OMPs cannot be detected at steady-state levels (9, 10).

The σ^E pathway detects periplasmic stress input and initiates a proteolytic cascade that results in the sequential degradation of the anti-sigma factor RseA (10). Unfolded OMPs bind the essential IM protease DegS and activate cleavage of the periplasmic domain of RseA (11-13). This stimulates degradation of the inner membrane region of RseA by RseP, resulting in the release of the cytoplasmic domain of the anti-sigma factor (14-17). The σ^E-bound cytoplasmic domain is then cleaved by ClpXP, freeing σ^E to transcribe its regulon (18-20). Included in the regulon are Bam complex members, chaperones, proteases, and small RNAs to repress expression of OMPs, among others (21, 22). Thus, activation of the σ^E response shifts the gene expression profile to improve the transport and assembly of OMPs, enhance the degradation of unfolded proteins that have aggregated in the periplasm, and slow the influx of precursor OMPs into the assembly pathway.

Regulation of the σ^E stress response pathway is critical to cell viability (23, 24). Constitutive activation of σ^E in the absence of stress, such as in the case of *rseA* null mutations, causes growth defects under standard culturing conditions (19, 25-28). The cell maintains control over σ^E activity through translational regulation; ribosomal profiling studies show that translation rates of RseA are much higher than those of σ^E (29, 30). The ability of the cell to turn

the σ^E pathway on in the presence of stress, shut it off when the threat subsides, and prevent activation in the absence of stress, is critical to cell survival (12, 31).

Here, we characterize an assembly-defective mutant of the maltoporin LamB that accumulates as an unfolded OMP substrate that is toxic under certain conditions. Selection for suppressors identified a novel mutation that alters the IM protease DegS and partially activates the σ^E stress response. This mutation also suppresses other distinct assembly-defective mutations, suggesting that the fine tuning of σ^E activity may have a significant impact on cell viability in otherwise toxic backgrounds.

Results

lamB$_{G439D}$ is an assembly-defective mutant

To investigate critical interactions that take place during OMP biogenesis, we perturbed the assembly process with a defective OMP substrate. We selected the maltoporin LamB as a candidate protein due to the ability to assay LamB assembly through maltodextrin utilization (32, 33). To impair assembly of LamB, we performed site-directed mutagenesis on a plasmid-encoded *lamB* under the control of a tetracycline-inducible promoter in order to avoid feedback from maltodextrin intake on the native promoter and assayed function in strains in which the native copy of *lamB* was deleted (34, 35). We selected a C-terminal conserved glycine at residue 439 for mutagenesis, as mutations of similarly positioned glycine residues have been shown to impair assembly of other OMPs (36-39). Residue G439 was mutated to either an alanine or a charge was introduced with an aspartate. To examine the effect of these mutations on LamB assembly, we assayed levels of monomeric and functional trimeric protein in cells grown at 30°C (Figure 1A). *lamB*$_{G439A}$ showed similar levels of monomeric and trimeric LamB as a control

strain expressing wild-type *lamB*, whereas $lamB_{G439D}$ exhibited drastically reduced levels of both forms of LamB. However, cells expressing $lamB_{G439D}$ form red colonies on MacConkey maltodextrin agar (Figure S1) and are able to grow in defined minimal maltodextrin media (Table S1), indicating that there is a small amount of functional protein assembled into the OM. We concluded that $LamB^{G439D}$, and not $LamB^{G439A}$, was assembly-defective, however, it remained unclear at what stage of assembly $LamB^{G439D}$ was impaired.

We hypothesized that the charge substitution could interfere with interactions with the Bam complex or with folding, as other previously described assembly-defective substrates exhibit defects at these stages in assembly (38-41). To determine if $LamB^{G439D}$ interacts aberrantly with the Bam complex, we measured the binding of LamB peptides encompassing residue 439 to the Bam complex using affinity co-purification (Figure 1B). We used binding to BamD as a measure of Bam complex engagement with the mutant substrate due to the role of BamD in recognizing OMPs (38, 40, 42). We first confirmed that residue 439 was located in a region of the protein that interacts with the Bam complex. LamB peptides encompassing residues 353-446 were able to bind BamD while peptides comprised of residues 26-121 did not co-purify with BamD, indicating that the protein region surrounding residue 439 binds to the Bam complex. Furthermore, we determined that LamB peptides (residues 353-446) containing G439A and G439D mutations bound to His-tagged BamD similarly to the wild type peptide, indicating that neither mutation changes the ability of LamB to engage with the Bam complex.

β-barrel proteins are resistant to denaturation by SDS alone, allowing the folding status of the protein to be assayed by comparing heat-denatured and non-denatured (incubated at room temperature) samples, a property called heat modifiability (43). Figure 1C shows heat modifiability of purified LamB following an *in vitro* folding assay. Purified $LamB^{+}$ and

LamB^{G439A} are folding-competent under non-denaturing conditions, evidenced by the appearance of folded molecules in non-denatured samples. However, no amount of folded LamB^{G439D} can be detected in the non-denatured samples. Taken together, we conclude that LamB^{G439D} is an assembly-defective mutant that is impaired in folding but not in recognition by the Bam complex.

Unfolded LamB^{G439D} is toxic in the absence of *degP*

Often, mutant OMP substrates fall off of the assembly pathway and misfold in the periplasm. Periplasmic proteases degrade the misfolded protein to prevent the toxicity associated with the accumulation of unfolded proteins (7, 8, 44). The folding defect of LamB^{G439D}, then, may make the assembly-defective protein a substrate of the periplasmic protease DegP. To examine this possibility, we deleted *degP* and monitored levels of monomeric and trimeric LamB^{G439D} in cells grown at 30°C (Figure 2A). Deletion of *degP* restored whole cell monomeric protein levels, supporting the model that LamB^{G439D} accumulates in the periplasm and is degraded by DegP. However, very little of the stabilized monomeric LamB^{G439D} is assembled into the OM, as evidenced by the minimal increase in functional LamB^{G439D} trimers (Figure 2A). The red colony phenotype on MacConkey maltodextrin agar and ability to grow in minimal maltodextrin media indicates that Δ*degP lamB*$_{G439D}$ cells do have functional LamB^{G439D} in the OM (Figure S1, Table S1). A protease-null mutant of *degP*, *degP*$_{S210A}$, also stabilizes levels of monomeric LamB^{G439D} (Figure 2B) (45). Thus, the absence of the DegP protease function stabilizes unfolded LamB^{G439D} monomers but the majority of this protein is not assembled into the OM.

Intriguingly, deletion of *degP* in a *lamB*$_{G439D}$ background is lethal at 37°C. To further demonstrate this conditional synthetic phenotype, we used genetic linkage analysis to quantify the frequency at which a *degP::*kan allele can be moved into the *lamB*$_{G439D}$ strain at 30°C and 37°C by co-transduction with a nearby *yadC::*Tn10 marker (Table 1). *degP*::kan can be moved into the *lamB*$_{G439D}$ strain at 30°C, albeit with some linkage disruption. However, the allele cannot be moved into the strain at the higher temperature, confirming that deletion of *degP* is synthetically lethal with *lamB*$_{G439D}$ at 37°C. We posit that the accelerated growth rate of cells at 37°C leads to a toxic aggregation of unfolded LamB^{G439D} that results in cell death.

Isolation of a suppressor of Δ*degP lamB*$_{G439D}$

We took advantage of the synthetic lethality of *lamB*$_{G439D}$ with *degP* deletion at 37°C to select for suppressors that restored assembly of the defective protein. To do this, we grew Δ*degP lamB*$_{G439D}$ cells at the permissive temperature of 30°C overnight, diluted the cultures, and plated on MacConkey maltodextrins at 37°C. This strategy allowed us to select for suppressors that both allowed viability of cells at the non-permissive temperature and screen for those that properly assembled LamB. Assembly of LamB was assayed using growth phenotype on the MacConkey maltodextrin agar; red colony color indicates that the cell assembled LamB and was able to take in maltodextrins (Figure S1) (46).

Most of the spontaneous suppressors restored growth at 37°C but did not restore assembly of LamB, resulting in white colonies on MacConkey maltodextrin agar. The high rate of suppressors that restored growth, but not assembly of LamB, suggests that they are *lamB* null mutations and this underscores the toxicity of LamB^{G439D}. We identified a chromosomal suppressor that was viable at both 30°C and 37°C and formed red colonies on MacConkey media

Journal of Bacteriology

supplemented with maltodextrins (Figure 3A). Using whole genome sequencing, we identified the *degS*$_{A323E}$ mutation and subsequently confirmed that this was a suppressor by marker rescue.

Immunoblot analysis showed that the suppressor mutation efficiently restored levels of trimeric LamB^{G439D} at 30°C and stabilized monomeric protein at 37°C (Figure 3C compare lanes 22-23, Figure 3B compare lanes 7-8). The suppressor mutation increased levels of LamB^{+}, LamB^{G439D}, and OmpA at higher temperatures (Figure 3B compare lanes 7-8, 13-14). However, it did not restore efficient trimer assembly of LamB^{G439D} (Figure 3C). This suggests that the *degS*$_{A323E}$ suppressor mutation both aids in the assembly of the mutant protein and ameliorates the toxicity of LamB^{G439D} in a temperature-dependent manner.

degS$_{A323E}$ increases basal levels of σ^E signaling

DegS^{A323E} contains an alanine-to-glutamate substitution at residue 323, which is located at the interface between the PDZ and protease domains of the protein (Figure 4A). Salt bridges at this interface stabilize the inactive conformation of DegS and are disrupted as a result of steric clashes upon OMP binding to the PDZ domain. Previous studies have shown that altering residues in the PDZ/protease domain interface changes the activity of DegS, likely through disruption of the salt bridge network (47-51). To assay DegS^{A323E} activity, we monitored σ^E activation through measurement of β-galactosidase activity from a σ^E-dependent *lacZ* reporter (Figure 4B-C) (52). *degS*$_{A323E}$ showed increased basal levels of σ^E activity in an otherwise isogenic, wild-type strain. This increase in σ^E activity was comparable to the levels of induction observed in a Δ*surA* strain but lower than activation in an *rseA* null, which exhibits fully active σ^E signaling (Figure 4B-C) (53, 54). However, *degS*$_{A323E}$ did prevent further induction when the σ^E response was induced. *degS*$_{A323E}$ Δ*surA* and *degS*$_{A323E}$ Δ*rseA* double mutants showed similar

levels of σ^E activation as Δ*surA* or Δ*rseA* mutants, respectively (Figure 4B-C). *degS*$_{A323E}$, then, primes the cell to handle stress with a higher basal level of σ^E activation, but this signaling is not further enhanced by DegS^{A323E} when stress is present.

To determine if elevated σ^E activity was sufficient for suppression, we tested if other mutations that increase levels of σ^E signaling could also suppress Δ*degP lamB*$_{G439D}$. Deletion of the anti-sigma factor *rseA* phenocopied the *degS*$_{A323E}$ suppressor; levels of trimeric LamB^{G439D} were more efficiently restored at 30°C and levels of the monomeric protein were stabilized at 37°C (Figure 3B). Removal of RseA, however, impacted cell viability and prevented robust growth on MacConkey maltodextrin agar even in wild-type strains (Figure S2). This is likely due to the toxic elevation of σ^E activity in cells lacking RseA (20) (25-28, 55).

In contrast, cells expressing *degS*$_{A323E}$ in an otherwise wild-type background grew similarly to wild-type cells both at 30°C and 37°C, indicating that the enhanced σ^E activity of this allele does not impact growth (Figure S3). Our data shows that multiple mutations that elevate σ^E activity can suppress Δ*degP lamB*$_{G439D}$ and suggests that the lowered activation of the *degS*$_{A323E}$ allele prevents the toxic effects of overactive stress signaling.

Increase in σ^E signaling by DegS^{A323E} suppresses many assembly-defective mutations

Previous studies show that elevated σ^E activity can alleviate the phenotypes of numerous assembly-defective conditions (56, 57). Because the σ^E stress response streamlines OMP biogenesis when the cell encounters stress, we wondered if *degS*$_{A323E}$ could suppress other assembly-defective conditions. We assayed suppression of *lptD*$_{Y721D}$ and Δ*bamB*Δ*bamE*, both of which impair OMP assembly and exhibit outer membrane defects (Figure 5). Importantly,

lptD$_{Y721D}$ and Δ*bamB*Δ*bamE* are defective at distinct stages of OMP assembly, allowing us to examine the scope of *degS*$_{A323E}$ suppression.

lptD$_{Y721D}$ is an assembly-defective mutant of LptD, the OM insertase of lipopolysaccharides, that exhibits an early folding defect and stalls on BamD during assembly. Due to the deficient interaction with BamD, LptD^{Y721D} falls off of the assembly pathway and is degraded in the periplasm. As such, *lptD*$_{Y721D}$ is characterized by reduced levels of folded LptD protein (41, 44). We hypothesized that increasing basal levels of σ^E signaling may alleviate this phenotype. We used Western blot analysis to detect reduced and oxidized LptD, representing unfolded and folded protein, respectively, in cells expressing both *degS*$_{A323E}$ and *lptD*$_{Y721D}$ (Figure 5A). We found that *degS*$_{A323E}$ increased levels of oxidized LptD^{Y721D}, indicating that more protein is assembled into the OM. This result shows that *degS*$_{A323E}$ suppresses multiple assembly-defective OMPs that are impaired at different stages of assembly.

Δ*bamB*Δ*bamE* is a conditionally lethal deletion of two lipoproteins in the Bam complex that results in global defects in OMP assembly. The drastic reduction in OMPs prevents growth of Δ*bamB*Δ*bamE* cells on rich media and at higher temperatures (58, 59). To determine if *degS*$_{A323E}$ could overcome a Bam complex mutant that impacts universal OMP assembly, we assayed growth of Δ*bamB*Δ*bamE* cells under non-permissive conditions (Figure 5B). In agreement with earlier studies, the Δ*bamB*Δ*bamE* double mutant grew only on minimal media. *degS*$_{A323E}$ suppressed this growth defect and restored the ability of Δ*bamB*Δ*bamE* to grow on rich media at higher temperatures. Taken together, our data shows that *degS*$_{A323E}$ is a powerful suppressor of several conditions that weaken the OM, including assembly-defective OMP substrates and Bam complex mutations.

Discussion

In this paper, we characterize *degS*$_{A323E}$, a novel mutation in the σ^E stress response pathway. This mutant was isolated as a suppressor of *lamB*$_{G439D}$, which specifies an assembly-defective mutant of the maltoporin LamB, also described here. LamB^{G439D} exhibits a folding defect that prevents robust assembly of functional protein into the OM. We show that deletion of *degP* stabilizes monomeric LamB^{G439D} at 30°C but is synthetically lethal with *lamB*$_{G439D}$ at 37°C, suggesting that unfolded monomeric protein accumulates in the absence of the protease (Figure 2A, Table 1). Removal of DegP only nominally increases levels of trimeric LamB^{G439D}, indicating that the majority of the monomeric protein that is stabilized in the absence of the protease is not assembled into the OM (Figure 2A).

We isolated *degS*$_{A323E}$ as a suppressor of Δ*degP lamB*$_{G439D}$ that both allowed viability at the non-permissive temperature and formation of red colonies on MacConkey maltodextrin agar (Figure 3A). We have shown that *degS*$_{A323E}$ increases basal levels of σ^E activation in otherwise wild-type strains without causing growth defects (Figure 4B, Figure S3). The partial σ^E activation exhibited by *degS*$_{A323E}$ is critical for viability; deletion of the anti-sigma factor *rseA* prevents robust growth on MacConkey agar containing maltodextrins (Figure S2). Strikingly, *degS*$_{A323E}$ also suppresses the assembly-defective mutations *lptD*$_{Y721D}$ and the conditional lethal phenotype of a Δ*bamB*Δ*bamE* double deletion strain (Figure 5). The partial activation of the σ^E stress response by *degS*$_{A323E}$ alleviated defects of these distinct assembly-defective conditions without creating toxicity associated with constitutively active σ^E activity.

We do not yet know the σ^E regulon member(s) directly responsible for the suppression of Δ*degP lamB*$_{G439D}$. At 30°C, the *degS*$_{A323E}$ suppressor mutation allows efficient assembly of functional LamB^{G439D} trimers. At elevated temperatures, however, the suppressor mutation

stabilizes monomeric LamB^{G439D} but does not allow efficient assembly of this protein into the OM (Figure 3B-C). Thus, *degS*$_{A323E}$ is able to both aid assembly of the mutant protein and ameliorate the toxicity of unfolded protein. We believe that *degS*$_{A323E}$ finely tunes the protein quality control network to achieve the balance between stabilization of unfolded protein and assembly into the OM. The increase in σ^E signaling in cells expressing *degS*$_{A323E}$ may result in changes in the expression of both proteases and chaperones. We think it is likely that even in the presence of *degS*$_{A323E}$, assembly of LamB^{G439D} does not occur at wild-type rates. At elevated temperatures, increased growth rates increase the load on the Bam complex and assembly of LamB^{G439D} is further compromised. It is not yet clear where the mutant protein is located in the cell, but it must be sequestered in some way that its toxicity is relieved. Identifying the key σ^E regulon members induced by *degS*$_{A323E}$ and the mechanism by which this shift in gene expression profile allows for enhanced assembly or reduced toxicity in the absence of assembly will require further study.

DegS forms a homotrimer, with each monomer comprised of a protease domain and a PDZ domain that binds unfolded OMPs. Under non-inducing conditions, DegS is maintained in an inactive state through autoinhibitory salt bridges at the PDZ/protease domain interface. Residues that are important for these stabilizing salt bridges include E317/R178, D320/R178, E324/K243, and D122/R256. Binding of an OMP causes a steric clash at the PDZ/protease domain interface, forcing conformational rearrangements that promote DegS activity through alignment of the catalytic triad (49-51, 60). Previously, it was shown that mutations that disrupt the autoinhibitory salt bridges or deletion of the PDZ domain altogether increase the basal activity of DegS (13, 47, 49, 51).

Residue 323 is located at the PDZ/protease domain interface and is directly adjacent to a residue that forms one of the stabilizing salt bridges that maintain the inactive conformation of the protein (D324) (49, 50). Substitution of a charged glutamate at this residue likely influences the salt bridge network that stabilizes the inactive protein in the wild-type protein. We found that DegS^{A323E} exhibits increased basal levels of σ^E signaling, suggesting that this amino acid change disrupts pre-existing salt bridges to bias the protein towards the active conformation. The increase in signaling was similar to that found in *surA* null strains. DegS^{A323E} is not fully activated, as evidenced the reduced σ^E signaling as compared to an *rseA* null mutant (Figure 4B). Thus, we believe that the system of salt bridges across the PDZ/protease domain interface is not disrupted, but rather the local network is weakened (47, 51).

degS$_{A323E}$, however, does not increase σ^E signaling under inducing conditions. We show that σ^E activation is equivalent in Δ*surA* and Δ*surA degS*$_{A323E}$ strains. The level of σ^E signaling in Δ*rseA* and Δ*rseA degS*$_{A323E}$ mutants are also comparable (Figure 4B). This is in agreement with an earlier study that shows that mutations of residues that contribute to the salt bridge network at the PDZ/protease domain interface increase levels of basal σ^E activity but do not further enhance activation in the presence of stress beyond that of wild-type DegS (51). We suggest that the disruption of the local network of salt bridges at the PDZ/protease domain interface in DegS^{A323E} increases basal levels activation of DegS^{A323E} but does not change the maximal activity of DegS^{A323E} compared to wild-type DegS when stress is present.

Our work shows that *degS*$_{A323E}$ is a powerful suppressor of a number of distinct conditions that disrupt the outer membrane, including *lamB*$_{G439D}$, *lptD*$_{Y721D}$, and Δ*bamB*Δ*bamE* (Figure 3, 5). Other studies have also demonstrated that enhanced σ^E stress response signaling, resulting from *rpoE* mutants or *rseA* null mutations, can suppress numerous assembly-defective

conditions (56, 57). We propose that *degS*$_{A323E}$ increases basal levels of σ^E signaling to prime the cell to respond to stress. Cell viability is ultimately determined by the race between escalating envelope stress and activation of stress response pathways. If left unchecked, the buildup of unfolded OMPs will reach toxic levels and kill the cell. Envelope stress response pathways detect unfolded OMP substrates and activate gene programs that counter the rapid accumulation of unfolded OMPs before they challenge cell viability. The increased levels of σ^E signaling exhibited by *degS*$_{A323E}$ prevent cell death by activating the protective σ^E regulon before the level of unfolded OMPs reaches lethal levels. Importantly, *degS*$_{A323E}$ lacks the growth defects characteristic of high levels of σ^E signaling (Figure S3) (25-28, 55). Therefore, we suggest that *degS*$_{A323E}$ finely tunes basal levels of σ^E activation to help the cell cope with stress associated with OMP assembly without creating the toxicity affiliated with high levels of σ^E activation.

Materials and Methods

Bacterial strains and plasmids

All strains, plasmids, and oligonucleotides used in this study are presented in Table S1. All oligonucleotides were ordered from Integrated DNA Technologies. Strains were constructed using standard microbiological techniques and grown as previously described (61). When necessary, LB media was supplemented with 20mg/L chloramphenicol, 25mg/L kanamycin (low), 50mg/L kanamycin (high), 50mg/L carbenicillin, or 10mg/L tetracycline. NovaBlue (Novagen), BL21(DE3) (Novagen), and Mach-1 (Thermo Fisher Scientific) strains were used for expression and cloning procedures. To evaluate suppression of Δ*bamB*Δ*bamE*, cultures were grown in M63 media supplemented with 0.2% glucose, 1mM $MgSO_4$, 100μg/mL thiamine, and a 500μL volume of LB. Unless otherwise noted, all strains were grown and constructed at 30°C.

Deletion alleles originated from the Keio Collection (28). In all strains, $degS_{A323E}$ was linked to the nearby *yhcG* Keio allele. Comparison of cells expressing $degS_{A323E}$ *yhcG*::kan was always made in reference to the isogenic control, which contained only *yhcG*::kan. When testing for suppression of Δ*bamB*Δ*bamE*, the *yhcG*::kan allele was removed by the use of FLP recombinase, as previously described (62). Growth phenotypes of wild-type Δ*bamB*, Δ*bamE*, and Δ*bamB*Δ*bamE* strains were not altered by Δ*yhcG* (Figure S4).

Western blot analysis

Overnight cultures were normalized by absorbance at 600nm (OD600). Samples were resuspended in the same volume of sample buffer containing β-ME. For oxidized blots, the sample buffer lacked β-ME. Samples were boiled for 10 minutes and subjected to electrophoresis through an SDS-PAGE gel (10% for LamB blots and 8% for LptD blots). Proteins were transferred to a nitrocellulose membrane (GE Healthcare, Amersham). Immunoblotting was performed using rabbit polyclonal antisera that recognizes LamB/OmpA/MBP (1:25,000), trimeric LamB (1:16,500), LptD (1:25,000), GroEL (1:10,000). Donkey anti-rabbit IgG horseradish peroxidase secondary antibody (GE Healthcare) was used at 1:10,000 dilution for all immunoblots.

Trimeric LamB sample preparation

Overnight cultures were normalized by OD600. Cells were resuspended in Bugbuster (Millipore), protease cocktail inhibitor (1:100, Sigma-Aldrich), benzonase (1:100, Sigma-Aldrich), and 1M $MgCl_2$ (1:100). Samples were lysed for 10 minutes at room temperature.

Laemelli sample buffer (Bio-Rad) supplemented with β-mercaptoethanol was added to dilute the sample volume 1:2. Samples were electrophoresed and analyzed as described above.

Preparation of biologically pure M63 minimal maltodextrin media

M63 media was supplemented with 80mL/L maltodextrin solution, 1mM $MgSO_4$, and 100μg/mL thiamine. MG2930 was inoculated into the media and grown overnight at 37°C. The cells were pelleted and the remaining supernatant was filtered (0.22μm pore, Millipore).

Growth phenotypes in minimal maltodextrin media

Strains were grown under permissive conditions in LB or LB supplemented with 20mg/L chloramphenicol, when appropriate. Cells were washed in M63 media and a normalized number of cells was inoculated into minimal maltodextrin media (containing 20mg/L chloramphenicol for plasmid maintenance, when necessary). After 24 hours of growth at 30°C, growth was scored.

Expression and Purification of Soluble BamD-His_6

Soluble BamD-His_6 was expressed from pCH86 in BL21(DE3) cells as described previously (42). Cultures were grown at 37°C to OD_{600} = 0.4, and then protein expression was induced by adding 0.1mM IPTG. The cultures were incubated for another 3-4 hours. The cells were collected by centrifugation at 5,000 x g for 10 minutes at 4°C and then resuspended in TBS (pH 8). They were lysed via cell disrupter and centrifuged again at 5,000 x g for 10 minutes at 4°C. Mechanical cell lysis was achieved using an EmulsiFlex-C3 cell disrupter (Avestin) at a pressure of 10,000 – 15,000 psi. The supernatant was collected and ultracentrifuged at 100,000 x

g for 30 minutes at 4°C. The clarified supernatant was then subjected to Ni-NTA affinity chromatography (Qiagen) followed by size exclusion chromatography (Superdex 200 column, GE Healthcare) in TBS (pH 8) (defined as 20mM Tris (pH 8) with 150mM NaCl unless otherwise noted).

Expression and Purification of wild-type/mutant LamB substrates and peptides

All full-length, truncated, and/or mutated forms of LamB were produced by expression in the cytoplasm of BL21(DE3) strains carrying the appropriate plasmid (pCH13, pJW384, pJW387, pJW410, pJW411, pJW412, pJW413, or pCH167). Cultures of these strains were grown at 37°C to OD_{600} = 0.4. Expression of the proteins was then induced by addition of 0.1mM IPTG, and the cultures were incubated for another 2-3 hours. The cells were then harvested, resuspended in TBS (pH 8) with added 0.1mg/mL deoxyribonuclease, 0.1mg/mL ribonuclease, 0.1 mg/mL lysozyme, and 1mM PMSF, and then lysed by cell disrupter. The cell lysates were centrifuged at 5,000 x g for 10 minutes at 4°C to pellet the inclusion bodies containing the LamB and BamA proteins or peptides. The inclusion bodies were washed once by resuspension in TBS (pH 8) and then centrifuged again at 5,000 x g for 10 minutes at 4°C. These inclusion bodies were dissolved in 8M urea by incubation with rocking at 25°C for approximately 30 minutes. The solutions were then centrifuged at 18,000 x g for 10 minutes at 4°C to pellet any undissolved material. These clarified urea solutions contained only minor amounts of other contaminating proteins as judged by SDS-PAGE and were used in the subsequent assays without further purification.

Affinity purifications with LamB or BamA peptides and folded BamD-His

Urea-denatured peptides were normalized to a concentration of 1mM in 8M urea (all protein concentrations were determined using the Bio-Rad DC Protein Assay) and diluted 10-fold into a TBS solution containing BamD-His, such that a final concentration of 50μM BamD-His and 100μM peptide was achieved. These solutions were incubated at room temperature for 20 minutes, upon which time 10μL was removed for "input samples". 80μL of the remaining sample was applied to 200μL Ni-NTA slurry (pre-equilibrated with TBS/20mM imidazole) and the resin was washed 2 x 1mL with TBS/20mM imidazole. The residual protein was eluted with 600μL of TBS/200mM imidazole, and 70μL of trichloroacetic acid was added to precipitate all protein components of the eluate. Following a 30 minute incubation on ice, the samples were centrifuged at 21,000 rcf for 10 minutes. The resulting protein pellets were resuspended in 20μL 1 M TRIS (pH 8), diluted 1:1 with 2X SDS sample buffer, and the samples were boiled for 5 minutes. Samples were analyzed via SDS-PAGE (200V, 45 minutes, 4μL input load, 2.5μL eluate load) followed by Coomassie staining.

Folding of wild-type or mutant LamB in detergent solution

Urea-denatured wild-type or mutant LamB was normalized to a concentration of 200μM in 8M urea and diluted ten-fold into 0.25% DDM (Anatrace)/20mM TRIS pH 8. The resulting solutions were rocked at room temperature for 20 hours. Samples were diluted 1:1 with 2x SDS-sample buffer and boiled (or not) for 5 minutes. The resulting samples were analyzed via semi-native SDS-PAGE (150V, 2 hours, 4°C, 4μL load).

Genetic linkage analysis

To quantitate selective pressure on deletion of *degP*, a *degP*::kan allele was introduced into strains by co-transduction with a nearby marker, *yadC*::Tn10. MC4100, BH191, BH290, and BH291 were infected with P1*vir* carrying both *degP*::kan and *yadC*::Tn10 at 30°C and 37°C. Tet^R transductants were selected (and Cat^R, where applicable). These transductants were then screened for Kan^R. The ratio of Kan^R transductants to total transductants screened was used to calculate co-transduction frequency. Transduction frequencies are a result 100 transductants screened each for three separate transductions.

Isolation of suppressor mutations

BH291 was grown at 30°C overnight in LB supplemented with 20mg/L chloramphenicol. Overnight cultures were diluted and plated on MacConkey media supplemented with 20mg/L chloramphenicol and 60mL/L maltodextrins. Plates were incubated overnight at 37°C. Colonies that were entirely red were streak purified onto MacConkey media supplemented with chloramphenicol and maltodextrins to ensure maintenance of the red growth phenotype. The background of the isolated suppressor was confirmed by colony PCR for *lamB* deletion and *degP* deletion, as well as cell death at 42°C to confirm *degP* deletion (63). The plasmid from the suppressor was isolated using the QIAprep Spin Miniprep Kit (Qiagen) and sequenced using Sanger sequencing (Genewiz Inc.) to screen for potential revertants. Finally, the suppressor plasmid was transformed into a clean background (BH273) to determine if the suppression was plasmid-linked or chromosomal. Only chromosomal suppressors were pursued. The $degS_{A323E}$ suppressor mutation described here was linked to a nearby genetic marker, *yhcG*::kan (28). This allowed the $degS_{A323E}$ allele to be moved into different strains by transduction, as previously described (61).

Whole genome sequencing sample preparation

A genomic DNA sample of KT26 was isolated using the DNeasy Blood and Tissue Kit (Qiagen), according to the manufacturer protocol described for Gram-negative organisms. An Illumina sequencing library of the genomic sample was prepared using the Nextera DNA library prep kit (Illumina, CA). The library was sequenced on an Illumina HiSeq 2500 sequencer with 75-nucleotide end-reads in accordance with the standard manufacturer protocol.

Whole genome sequencing analysis

Demultiplexed reads were assembled using the SPAdes genome assembly algorithm (64). The assembled genome was then aligned to a reference genome (*Escherichia coli* K-12 NC_000913.3) using the Mauve multiple genome alignment program (65, 66). Nucleotide changes in the suppressor genome (KT26) relative to the reference genome were identified, and mutations were confirmed by Sanger sequencing of PCR amplified loci (Genewiz Inc.).

β-galactosidase assay

Overnight cultures were diluted 1:100 in fresh LB and grown until late exponential phase (OD600 ~.8-1.0). Samples were normalized by OD600, pelleted, and resuspended in the same volume of Z buffer (60mM Na_2HPO_4, 40mM NaH_2PO_4, 10mM KCl, 1mM $MgSO_4$, 50mM β-ME). 30μL of 0.1% SDS and a 50μL volume of chloroform was added. Samples were vortexed for 10 seconds each and left to lyse for 10 minutes. A 100μL volume of each cell lysate was mixed with 50μL of 4mg/mL ONPG (O-nitrophenyl-β-D-galactopyranoside) solution in Z buffer. β-galactosidase activity was analyzed by kinetic measurement of OD420 in a Bio Tek Synergy 1

plate reader and V_{max} was determined using Gen5 software. Experiments were performed in three biological replicates and mean values +/- standard error of the mean (SEM) were plotted. Significance was determined by a *t*-test.

Efficiency of plating (EOP) assay

Overnight cultures were normalized by absorbance at 600nm (OD600). For assaying Δ*bamB*Δ*bamE* viability, 10-fold dilutions were made in minimal glucose and replica plated onto LB or minimal glucose plates and incubated at 30°C and 37°C.

Growth curves

Overnight cultures were normalized by absorbance at 600nm (OD600). Cells were inoculated into 2mL fresh LB in a 24-well microtiter plate (Corning no. 3526). Cultures were grown at 37°C with aeration in a BioTek Synergy H1 plate reader for 16 hours. Growth curves were performed in biological triplicate and mean values +/- standard deviation were plotted.

Acknowledgements

We would like to thank current and former members of the T.J.S. and D.K. laboratories for helpful discussion and Wei Wang and Jessica Wiggins at the Lewis-Sigler Institute Genomics Core Facility of Princeton University for performing the whole-genome sequencing. We would also like to thank Rajeev Misra for sharing unpublished data and productive conversation. Research reported in this publication was supported by the National Institute of General Medicine Sciences of the National Institutes of Health under grant number R35-GM118024 and R01-GM034821 (to T.J.S.) T32-GM007388 (to Princeton University- E.M.H) and the National

Institute of Allergy and Infectious Disease of the National Institute of Health under grant number R01-AI081059 (to D.K.). The content is solely the responsibility of the authors and does not necessarily represent the official views of the National Institutes of Health.

Author contributions: E.M.H, A.O'C., J.W., D.K., and T.J.S. designed the research. E.M.H, K.T., M.G., and J.W. performed the research. E.M.H and T.J.S. wrote the paper.

References

1. **Silhavy TJ**, **Kahne D**, **Walker S**. 2010. The Bacterial Cell Envelope. Cold Spring Harbor Perspectives in Biology **2**:a000414–a000414.

2. **Nikaido H**, **Vaara M**. 1992. Molecular Basis of Bacterial Outer Membrane Permeability. Microbiological Reviews **49**:1–32.

3. **Plessis du DJF**, **Nouwen N**, **Driessen AJM**. 2011. The Sec translocase. BBA - Biomembranes **1808**:851–865.

4. **Beckwith J**. 2013. The Sec-dependent pathway. Research in Microbiology **164**:497–504.

5. **Hagan CL**, **Silhavy TJ**, **Kahne D**. 2011. β-Barrel Membrane Protein Assembly by the Bam Complex. Annu Rev Biochem **80**:189–210.

6. **Konovalova A**, **Kahne D**, **Silhavy TJ**. 2017. Outer Membrane Biogenesis. Annu Rev Microbiol **71**:539–556.

7. **Merdanovic M**, **Clausen T**, **Kaiser M**, **Huber R**, **Ehrmann M**. 2011. Protein Quality Control in the Bacterial Periplasm. Annu Rev Microbiol **65**:149–168.

8. **Konovalova A**, **Grabowicz M**, **Balibar CJ**, **Malinverni JC**, **Painter RE**, **Riley D**, **Mann PA**, **Wang H**, **Garlisi CG**, **Sherborne B**, **Rigel NW**, **Ricci DP**, **Black TA**, **Roemer T**, **Silhavy TJ**, **Walker SS**. 2018. Inhibitor of intramembrane protease RseP blocks the σ^E response causing lethal accumulation of unfolded outer membrane proteins. Proc Natl Acad Sci USA **15**:201806107–8.

9. **Ades SE**. 2008. Regulation by destruction: design of the σ^E envelope stress response. Current Opinion in Microbiology **11**:535–540.

10. **Barchinger SE**, **Ades SE**. 2013. Regulated Proteolysis: Control of the *Escherichia coli* σ^E-Dependent Cell Envelope Stress Response, pp. 129–160. *In* Regulated Proteolysis in Microorganisms. Springer Netherlands, Dordrecht.

11. **Struyve M**, **Moons M**, **Tommassen J**. 1991. Carboxy-terminal Phenylalanine is Essential for the Correct Assembly of a Bacterial Outer Membrane Protein. Journal of Molecular Biology 141–148.

12. **Alba BM**, **Zhong HJ**, **Pelayo JC**, **Gross CA**. 2001. *degS* (*hhoB*) is an essential *Escherichia coli* gene whose indispensable function is to provide σ^E activity. Mol Microbiol **40**:1323–1333.

13. **Walsh NP**, **Alba BM**, **Bose B**, **Gross CA**, **Sauer RT**. 2003. OMP Peptide Signals Initiate the Envelope-Stress Response by Activating DegS Protease via Relief of Inhibition Mediated by Its PDZ Domain. Cell **113**:61–71.

14. **Alba BM**, **Leeds JA**, **Onufryk C**, **Lu CZ**, **Gross CA**. 2002. DegS and YaeL participate sequentially in the cleavage of RseA to activate the sigma E-dependent extracytoplasmic stress response. Genes and Development **16**:2156–2168.

15. **Kanehara K**, **Ito K**, **Akiyama Y**. 2002. YaeL (EcfE) activates the σ^E pathway of stress response through a site-2 cleavage of anti-σ^E, RseA. Genes and Development **16**:2147–2155.

16. **Kanehara K**, **Ito K**, **Akiyama Y**. 2003. YaeL proteolysis of RseA is controlled by the PDZ domain of YaeL and a Gln-rich region of RseA. EMBO **22**:6839–6398.

17. **Akiyama Y**, **Kanehara K**, **Ito K**. 2004. RseP (YaeL), an Escherichia coli RIP protease, cleaves transmembrane sequences. EMBO **23**:4434–4442.

18. **Flynn JM**, **Levchenko I**, **Sauer RT**, **Baker TA**. 2004. Modulating substrate choice: the SspB adaptor delivers a regulator of the extracytoplasmic-stress response to the AAA+ protease ClpXP for degradation. Genes and Development **18**:2292–2301.

19. **Missiakas D**, **Mayer MP**, **Lemaire M**, **Georgopoulos C**, **Raina S**. 1997. Modulation of the *Escherichia coli* σ^E (RpoE) heat-shock transcription-factor activity by the RseA, RseB, and RseC proteins. Mol Microbiol **24**:355–371.

20. **Ades SE**, **Connolly LE**, **Alba BM**, **Gross CA**. 1999. The *Escherichia coli* σ^E-dependent extracytoplasmic stress response is controlled by the regulated proteolysis of an anti-σ factor. Genes and Development **13**:2449–2461.

559 21. **Rhodius VA**, **Suh WC**, **Nonaka G**, **West J**, **Gross CA**. 2005. Conserved and Variable
560 Functions of the σ^E Stress Response in Related Genomes. PLoS Biology **4**:e2–17.

561 22. **Johansen J**, **Rasmussen AA**, **Overgaard M**, **Valentin-Hansen P**. 2006. Conserved
562 Small Non-coding RNAs that belong to the σ^E Regulon: Role in Down-regulation of Outer
563 Membrane Proteins. Journal of Molecular Biology **364**:1–8.

564 23. **Las Peñas de A**, **Connolly L**, **Gross CA**. 1997. σ^E Is an Essential Sigma Factor in
565 *Escherichia coli*. Journal of Bacteriology **179**:6862–6864.

566 24. **Hayden JD**, **Ades SE**. 2008. The Extracytoplasmic Stress Factor, σ^E, Is Required to
567 Maintain Cell Envelope Integrity in *Escherichia coli*. PLoS ONE **3**:e1573–13.

568 25. **Nitta T**, **Nagamitsu H**, **Murata M**, **Izu H**, **Yamada M**. 2000. Function of the σ^E
569 Regulon in Dead-Cell Lysis in Stationary-Phase *Escherichia coli*. Journal of Bacteriology
570 **182**:5231–5237.

571 26. **Noor R**, **Murata M**, **Nagamitsu H**, **Klein G**, **Raina S**, **Yamada M**. 2009. Dissection of
572 σ^E-dependent cell lysis in *Escherichia coli*: roles of RpoE regulators RseA, RseB and
573 periplasmic folding catalyst PpiD. Genes to Cells **14**:885–899.

574 27. **Kabir MS**. 2005. Cell lysis directed by σ^E in early stationary phase and effect of induction
575 of the *rpoE* gene on global gene expression in *Escherichia coli*. Microbiology **151**:2721–
576 2735.

28. **Baba T**, **Ara T**, **Hasegawa M**, **Takai Y**, **Okumura Y**, **Baba M**, **Datsenko KA**, **Tomita M**, **Wanner BL**, **Mori H**. 2006. Construction of *Escherichia coli* K-12 in-frame, single-gene knockout mutants: the Keio collection. Mol Syst Biol **2**:473–11.

29. **Ades SE**, **Grigorova IL**, **Gross CA**. 2003. Regulation of the Alternative Sigma Factor σ^E during Initiation, Adaptation, and Shutoff of the Extracytoplasmic Heat Shock Response in *Escherichia coli*. Journal of Bacteriology **185**:2512–2519.

30. **Li G-W**, **Burkhardt D**, **Gross C**, **Weissman JS**. 2014. Quantifying Absolute Protein Synthesis Rates Reveals Principles Underlying Allocation of Cellular Resources. Cell **157**:624–635.

31. **Hayden JD**, **Ades SE**. 2008. The Extracytoplasmic Stress Factor, σ^E, Is Required to Maintain Cell Envelope Integrity in *Escherichia coli*. PLoS ONE **3**:e1573–13.

32. **Szmelcman S**, **Hofnung M**. 1975. Maltose Transport in *Escherichia coli* K-12: Involvement of the Bacteriophage Lambda Receptor. Journal of Bacteriology **124**:112–118.

33. **Wang Y-F**, **Dutzler R**, **Rizkallah PJ**, **Rosenbusch JP**, **Schirmer T**. 1997. Channel Specificity: Structural Basis for Sugar Discrimination and Differential Flux Rates in Maltoporin. Journal of Molecular Biology **272**:56–63.

34. **Cole ST**, **Raibaud O**. 1986. The nucleotide sequence of the *malT* gene encoding the positive regulator of the *Escherichia coli* maltose regulon. Gene **42**:201–208.

35. **Raibaud O**, **Vidal-Ingigliardi D**, **Richet E**. 1989. A Complex Nucleoprotein Structure Involved in Activation of Transcription of Two Divergent *Escherichia coli* Promoters. Journal of Molecular Biology **205**:471–485.

36. **Robert V**, **Volokhina EB**, **Senf F**, **Bos MP**, **Van Gelder P**, **Tommassen J**. 2006. Assembly Factor Omp85 Recognizes Its Outer Membrane Protein Substrates by a Species-Specific C-Terminal Motif. PLoS Biology **4**:e377.

37. **Kutik S**, **Stojanovski D**, **Becker L**, **Becker T**, **Meinecke M**, **Krüger V**, **Prinz C**, **Meisinger C**, **Guiard B**, **Wagner R**, **Pfanner N**, **Wiedemann N**. 2008. Dissecting Membrane Insertion of Mitochondrial β-Barrel Proteins. Cell **132**:1011–1024.

38. **Hagan CL**, **Wzorek JS**, **Kahne D**. 2015. Inhibition of the β-barrel assembly machine by a peptide that binds BamD. Proc Natl Acad Sci USA **112**:2011–2016.

39. **Wzorek JS**, **Lee J**, **Tomasek D**, **Hagan CL**, **Kahne D**. 2017. Membrane integration of an essential β-barrel protein prerequires burial of an extracellular loop. Proc Natl Acad Sci USA **114**:2598–2603.

40. **Lee J**, **Xue M**, **Wzorek JS**, **Wu T**, **Grabowicz M**, **Gronenberg LS**, **Sutterlin HA**, **Davis RM**, **Ruiz N**, **Silhavy TJ**, **Kahne D**. 2016. Characterization of a stalled complex on the β-barrel assembly machine. Proc Natl Acad Sci USA **113**:8717–8722.

41. **Lee J**, **Sutterlin HA**, **Wzorek JS**, **Mandler MD**, **Hagan CL**, **Grabowicz M**, **Tomasek D**, **May MD**, **Hart EM**, **Silhavy TJ**, **Kahne D**. 2018. Substrate binding to BamD triggers a conformational change in BamA to control membrane insertion. Proc Natl Acad Sci USA **115**:2359–2364.

42. **Hagan CL**, **Westwood DB**, **Kahne D**. 2013. Bam Lipoproteins Assemble BamA in Vitro. Biochemistry **52**:6108–6113.

43. **Noinaj N**, **Kuszak AJ**, **Buchanan SK**. 2015. Heat Modifiability of Outer Membrane Proteins from Gram-Negative Bacteria, pp. 51–56. *In* Protein Nanotechnology. Springer New York, New York, NY.

44. **Soltes GR**, **Martin NR**, **Park E**, **Sutterlin HA**, **Silhavy TJ**. 2017. Distinctive Roles for Periplasmic Proteases in the Maintenance of Essential Outer Membrane Protein Assembly. Journal of Bacteriology **199**:e00418–17–10.

45. **Speiss C**, **Beil A**, **Ehrmann M**. 1999. A Temperature-Dependent Switch from Chaperone to Protease in a Widely Conserved Heat Shock Protein. Cell **97**:1339–3479.

46. **Shuman HA**, **Silhavy TJ**. 2003. THE ART AND DESIGN OF GENETIC SCREENS: *ESCHERICHIA COLI*. Nature Reviews Genetics **4**:419–431.

47. **Mauldin RV**, **Sauer RT**. 2012. Allosteric regulation of DegS protease subunits through a shared energy landscape. Nat Chem Biol **9**:90–96.

48. **Sohn J**, **Sauer RT**. 2009. OMP Peptides Modulate the Activity of DegS Protease by Differential Binding to Active and Inactive Conformations. Molecular Cell **33**:64–74.

49. **Wilken C**, **Kitzing K**, **Kurzbauer R**, **Ehrmann M**, **Clausen T**. 2004. Crystal Structure of the DegS Stress Sensor: How a PDZ Domain Recognizes Misfolded Protein and Activates a Protease. Cell **117**:483–494.

636 50. **Zeth K**. 2004. Structural analysis of DegS, a stress sensor of the bacterial periplasm.
637 FEBS Letters **569**:351–358.

638 51. **Sohn J**, **Grant RA**, **Sauer RT**. 2007. Allosteric Activation of DegS, a Stress Sensor PDZ
639 Protease. Cell **131**:572–583.

640 52. **Button JE**, **Silhavy TJ**, **Ruiz N**. 2007. A suppressor of cell death caused by the loss of σ^E
641 downregulates extracytoplasmic stress responses and outer membrane vesicle production
642 in *Escherichia coli*. Journal of Bacteriology **189**:1523–1530.

643 53. **Missiakas D**, **Betton J-M**, **Raina S**. 1996. New components of protein folding in
644 extracytoplasmic compartments of *Escherichia coli* SurA, FkpA and Skp/OmpH. Mol
645 Microbiol **21**:871–884.

646 54. **Rouvière PE**, **Gross CA**. 1996. SurA, a periplasmic protein with peptidyl-prolyl
647 isomerase activity, participates in the assembly of outer membrane porins. Genes and
648 Development **10**:3170–3182.

649 55. **Nicoloff H**, **Gopalkrishnan S**, **Ades SE**. 2017. Appropriate Regulation of the σ^E-
650 Dependent Envelope Stress Response Is Necessary To Maintain Cell Envelope Integrity
651 and Stationary-Phase Survival in *Escherichia coli*. Journal of Bacteriology **199**:203–17.

652 56. **Leiser OP**, **Charlson ES**, **Gerken H**, **Misra R**. 2012. Reversal of the Δ*degP* Phenotypes
653 by a Novel *rpoE* Allele of *Escherichia coli*. PLoS ONE **7**:e33979–8.

57. **Konovalova A**, **Schwalm JA**, **Silhavy TJ**. 2016. A Suppressor Mutation That Creates a Faster and More Robust σ^E Envelope Stress Response. Journal of Bacteriology **198**:2345–2351.

58. **Sklar JG**, **Wu T**, **Gronenberg LG**, **Malinverni JC**, **Malinverni J**, **Kahne D**, **Silhavy TJ**. 2007. Lipoprotein SmpA is a component of the YaeT complex that assembles outer membrane proteins in *Escherichia coli*. Proc Natl Acad Sci USA **104**:6400–6405.

59. **Tellez R**, **Misra R**. 2011. Substitutions in the BamA β-Barrel Domain Overcome the Conditional Lethal Phenotype of a Δ*bamB bamE* Strain of *Escherichia coli*. Journal of Bacteriology **194**:317–324.

60. **de Regt AK**, **Baker TA**, **Sauer RT**. 2015. Steric clashes with bound OMP peptides activate the DegS stress-response protease. Proc Natl Acad Sci USA **112**:3326–3331.

61. **Silhavy TJ**, **Berman ML**, **Enquist LW**. Experiments with Gene Fusions. Cold Spring Harbor Laboratory.

62. **Datsenko KA**, **Wanner BL**. 2000. One-step inactivation of chromosomal genes in *Escherichia coli* K-12 using PCR products. Proc Natl Acad Sci USA **97**:6640–6645.

63. **Lipinska B**, **Zylicz M**, **Georgopoulos C**. 1990. The HtrA (DegP) Protein, Essential for *Escherichia coli* Survival at High Temperatures, Is an Endopeptidase. Journal of Bacteriology **172**:1791–1797.

64. **Bankevich A**, **Nurk S**, **Antipov D**, **Gurevich AA**, **Dvorkin M**, **Kulikov AS**, **Lesin VM**, **Nikolenko SI**, **Pham S**, **Prjibelski AD**, **Pyshkin AV**, **Sirotkin AV**, **Vyahhi N**, **Tesler G**,

Alekseyev MA, **Pevzner PA**. 2012. SPAdes: A New Genome Assembly Algorithm and Its Applications to Single-Cell Sequencing. Journal of Computational Biology **19**:455–477.

65. **Darling AC**, **Mau B**, **Blattner FR**, **Perna NT**. 2004. Mauve: Multiple Alignment of Conserved Genomic Sequence With Rearrangements. Genome Research **14**:1394–1403.

66. **Edwards DJ**, **Holt KE**. 2013. Beginner's guide to comparative bacterial genome analysis using next-generation sequence data. Microbial Informatics and Experimentation **3**:1–9.

Tables and Figure Legends

Table 1: *degP* deletion is synthetically lethal with *lamB*$_{G439D}$ at 37°C.

Recipient strain	*degP*::kan *yadC*::Tn10 cotransduction frequency (%)*	
	30°C	37°C
MC4100	50	44
Δ*lamB*	53	47
Δ*lamB* p*lamB*$^{+}$	53	40
Δ*lamB* p*lamB*$_{G439D}$	27	<1

*P1*vir* lysates carrying *degP*::kan *yadC*::Tn10 were transduced into the indicated strains at the designated temperature. The Tet^{R} transductants were then tested for Kan^{R} to calculate co-transduction of *degP*::kan and *yadC*::Tn10 markers. Co-transduction frequency represents three separate transductions.

Figure 1: LamB^{G439D} is a folding-defective mutant. (A) Monomeric and trimeric LamB levels were determined in strains with the genotypes listed by SDS-PAGE and immunoblotting.

Antibodies specific to the monomeric and trimer protein were used. **(B)** Purified LamB peptides were incubated with His-tagged BamD and co-immunoprecipitated and analyzed by SDS-PAGE analysis. **(C)** Purified LamB protein was boiled (denatured) or incubated at room temperature (non-denatured) and examined by electrophoresis.

Figure 2: The absence of DegP protease function stabilizes monomeric LamB^{G439D} at 30°C. Monomeric or trimeric LamB was detected using whole cell lysates made from strains of the listed genotypes, in Δ*degP* or *degP$_{S210A}$ yadC::*Tn10 backgrounds, and analyzed by SDS-PAGE and immunoblotting. Antibodies that specifically detect monomeric and trimer LamB were used.

Figure 3: ***degS$_{A323E}$* suppresses *lamB$_{G439D}$*. (A)** The indicated strains were streaked onto MacConkey maltodextrin indicator agar at 37°C. Strains not carrying the plasmid-encoded *lamB* carry an empty vector control. **(B)** Whole cell lysates of the indicated strains were analyzed by SDS-PAGE and immunoblotting. Monomeric and trimeric LamB was detected using antibodies specific for those protein conformations. Unless otherwise indicated, the strains were grown at 30°C.

Figure 4: *degS$_{A323E}$* partially activates basal levels of σ^E signaling. (A) DegS^{A323} (red) is located at the PDZ/protease domain interface of DegS. These domains interact by a number of salt bridges (teal) that stabilize the inactive conformation of the protein. Dashed lines indicate polar contacts. Image was generated from the peptide-free structure of DegS (PDB: 1SOT) (49). **(B-C)** Measurement of the Vmax of β-galactosidase activity driven from *rpoH*P3, a σ^E-dependent promoter, in the indicated strains (52). Graphs are plotted +/- standard error of the

mean (SEM), *n=3*. Significance was calculated using a *t* test. Strains were grown at **(B)** 37°C and **(C)** 30°C.

Figure 5: *degS*$_{A323E}$ suppresses multiple assembly-defective mutations. (A) Immunoblot analysis of whole cell lysates to detect relative levels of LptD. Oxidized samples ("ox") were lysed with sample buffer lacking β-ME, while reduced samples ("red") were lysed with sample buffer containing β-ME. Levels of GroEL served as a loading control. **(B)** An efficiency of plating assay was performed by spotting 10-fold dilutions of overnight cultures onto LB and minimal glucose plates. Plates were incubated at the indicated temperature.

Journal of Bacteriology

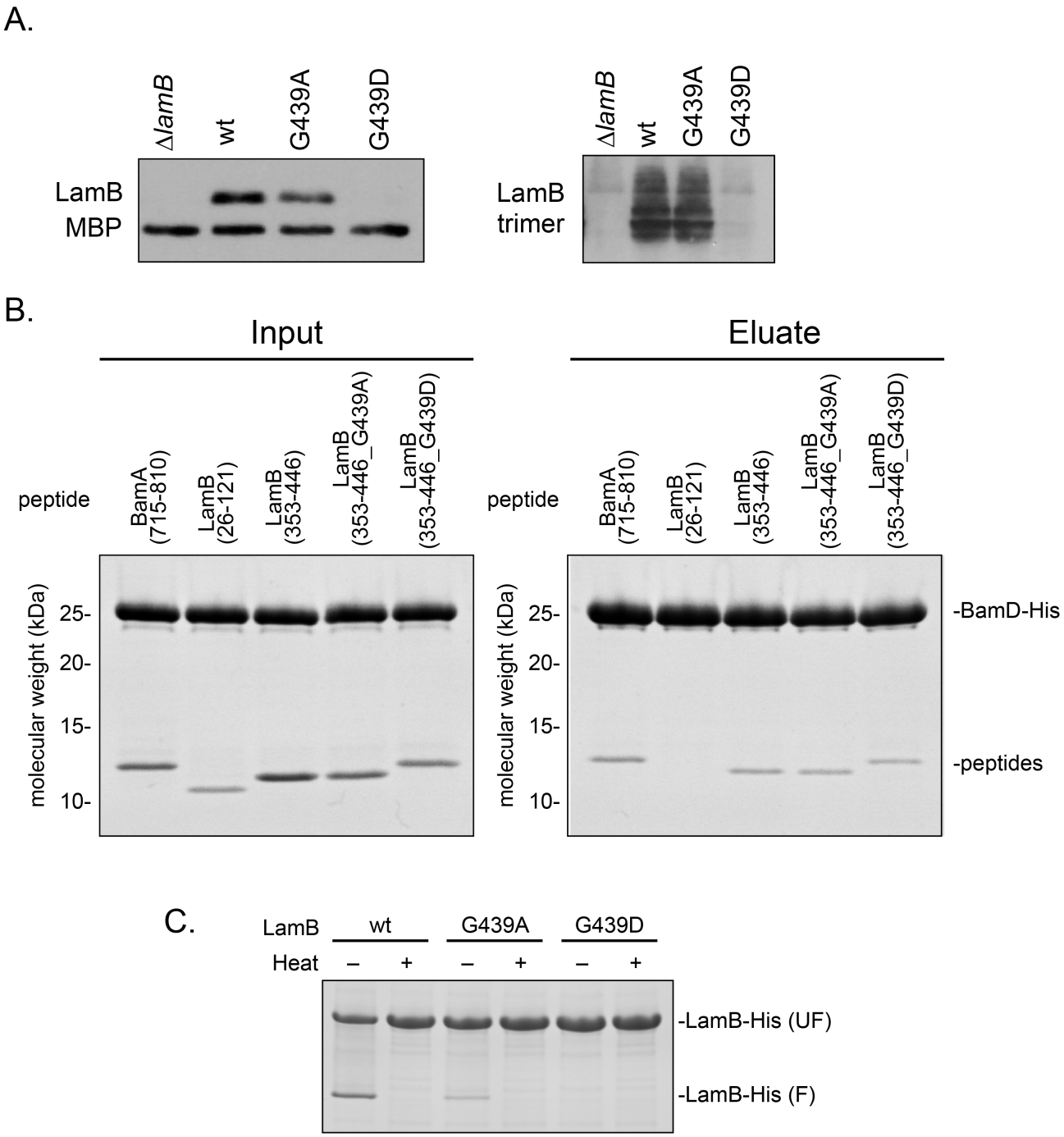

A.

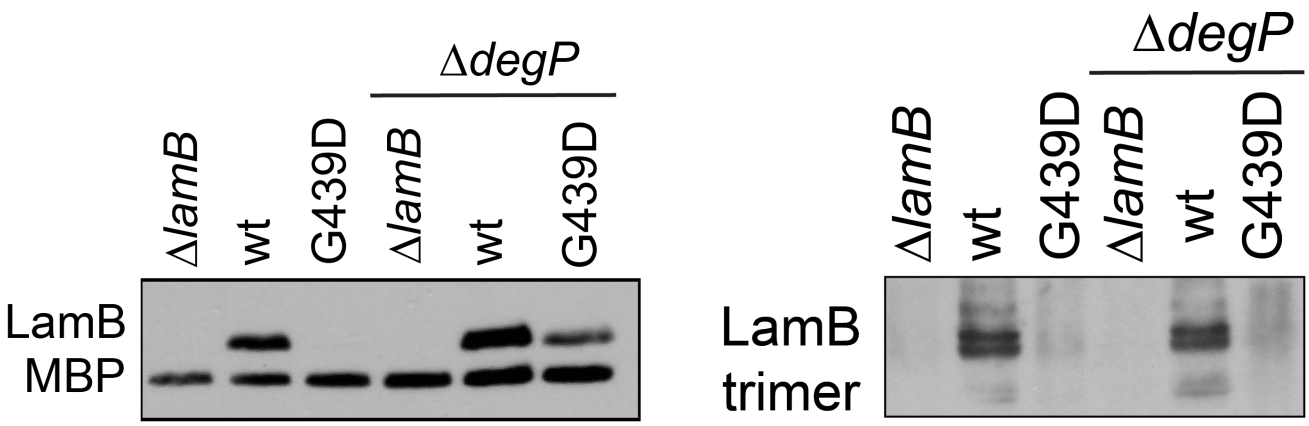

B.

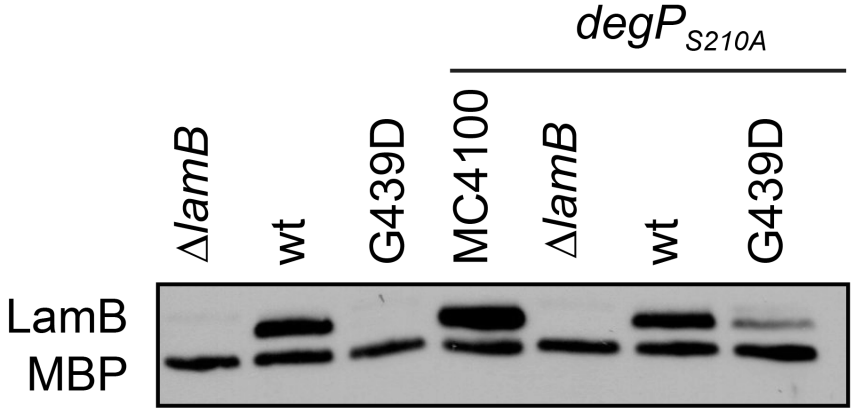

A.

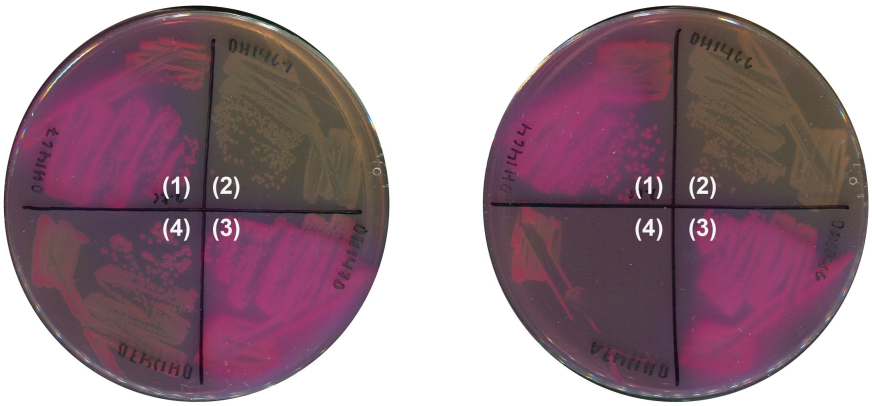

(1) MC4100 *degS*$_{A323E}$
(2) Δ*lamB* Δ*degP degS*$_{A323E}$
(3) Δ*lamB* Δ*degP plamB degS*$_{A323E}$
(4) Δ*lamB* Δ*degP plamB*$_{G439D}$ *degS*$_{A323E}$

(1) MC4100
(2) Δ*lamB* Δ*degP*
(3) Δ*lamB* Δ*degP plamB*
(4) Δ*lamB* Δ*degP plamB*$_{G439D}$

B.

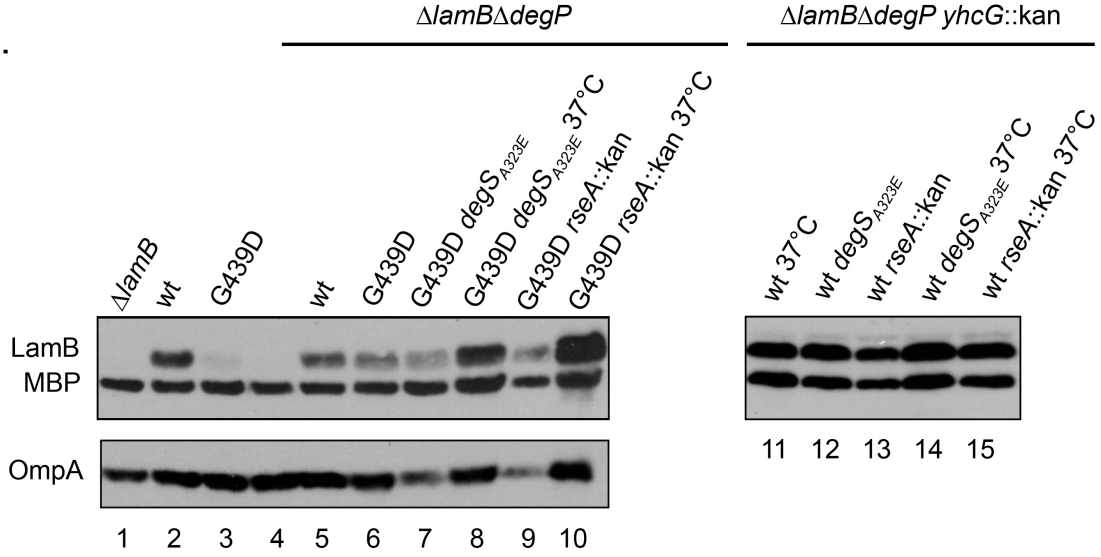

C.